



ELSEVIER

doi:10.1016/j.gca.2004.09.007

Highly siderophile element geochemistry of ^{187}Os -enriched 2.8 Ga Kostomuksha komatiites, Baltic Shield

IGOR S. PUCHTEL^{*,†} and MUNIR HUMAYUN[‡]

Department of the Geophysical Sciences, The University of Chicago, 5734 S. Ellis Avenue, Chicago, Illinois 60637, USA

(Received April 9, 2004; accepted in revised form September 3, 2004)

Abstract—New analyses of highly siderophile elements (HSE; Re, Os, Ir, Ru, Pt, and Pd) obtained by Carius tube digestion isotope dilution inductively coupled plasma mass-spectrometry (ID-ICPMS) technique are reported for ^{187}Os -enriched 2.8 Ga komatiites from the Kostomuksha greenstone belt. As a result of a significant improvement in the yield over our previous digestions by the NiS fire-assay technique, these komatiites have now been shown to contain 22 to 25% more Os, Ir, and Pt and 34% more Ru. The emplaced komatiite lavas at Kostomuksha thus had siderophile element abundances comparable to those of the Abitibi belt. The discrepancies observed between the two techniques are interpreted to be the result of incomplete digestion of HSE carriers (particularly chromite) during the NiS fire-assay procedure. Our results for UB-N peridotite reference material agree well with those obtained by the high-pressure ashing digestion ID-ICPMS technique reported in the literature. Two types of komatiite lavas have been distinguished in this study based on the IPGE (Os, Ir, and Ru) behavior during lava differentiation. The Kostomuksha type is unique and is characterized by an incompatible behavior of IPGEs, with bulk solid-liquid partition coefficients for IPGEs being close to those for olivine. Cumulate zones in this type of komatiite lava occupy <20% of the total thickness of the flows. The Munro type exhibits a compatible behavior of IPGEs during lava differentiation. The cumulate zone in this type of komatiite occupies >20% of the total thickness of the flows. The calculated bulk partition coefficients indicate that, as with the other Munro-type komatiite lavas, the bulk cumulate contained an IPGE-rich minor phase(s) in addition to olivine. The non-CI chondritic HSE pattern for the source of the Kostomuksha komatiites calculated here is similar to that of Abitibi komatiites and to average depleted spinel lherzolite (ADSL) and supports the hypothesis of a non-CI chondritic HSE composition of the Earth's mantle. The absolute HSE abundances in the source of the Kostomuksha komatiite have been demonstrated to be comparable to those of the source of Abitibi komatiites, even though the two komatiites contrast in their Os isotopic compositions. This supports the earlier hypothesis that if core-mantle interaction produced the $^{187}\text{Os}/^{188}\text{Os}$ radiogenic signature in the Kostomuksha source, it must have occurred in the form of isotope exchange at the core-mantle boundary. Other explanations of the radiogenic Os signature are similarly constrained to conserve the elemental abundance pattern in the mantle source of Kostomuksha komatiites. Copyright © 2005 Elsevier Ltd

1. INTRODUCTION

The 2.8 Ga Kostomuksha greenstone belt is one of the few Archean komatiitic lava suites on Earth that were shown to have been derived from a mantle source with radiogenic initial $^{187}\text{Os}/^{188}\text{Os}$ isotopic composition (Puchtel et al., 2001; Walker and Nisbet, 2002). These lavas provide the type of material that can be used to test models of core-mantle interaction and oceanic crust recycling through studying variations in highly siderophile element (HSE; Re, Os, Ir, Ru, Pt, and Pd) abundances in mantle sources of these lavas, and of those that exhibit near-chondritic initial $^{187}\text{Os}/^{188}\text{Os}$ isotopic compositions, such as Alexo (Gangopadhyay and Walker, 2003) and Pyke Hill komatiites (Puchtel et al., 2004a) in Canada. These tests require an accurate determination of HSE abundances in the emplaced lavas.

Puchtel and Humayun (2000) reported platinum group ele-

ment (PGE) abundances in komatiitic and basaltic lavas from the Kostomuksha greenstone belt analyzed by the NiS fire-assay digestion isotope dilution inductively coupled plasma mass-spectrometry (ID-ICPMS) technique. These PGE data were used to infer the PGE abundances in the mantle source of the lavas to test models of ocean crust recycling and core-mantle interaction. Subsequently, the NiS fire-assay technique was shown to be inefficient at digesting some PGE carriers in komatiitic samples (Puchtel et al., 2004b). Due to these shortcomings, abundances of some PGEs in the lavas were shown to be underestimated by as much as 50%. This, in turn, results in underestimation of PGE abundances in the mantle source of the lavas and may have broader impact on several important conclusions in that study, including the incompatible behavior of Os and Ir during lava differentiation.

The Carius tube (CT) digestion technique (Shirey and Walker, 1995) has been recently demonstrated to be superior to the NiS fire-assay method in digesting PGE carriers in komatiites (Puchtel et al., 2004b). In this paper, we present new CT digestion, ID-ICPMS analyses of PGEs and Re in the complete set of eighteen drill core samples from seven komatiite lava flows from the Puchtel and Humayun (2000) study, as well as in nine additional samples from the same lava flows, including

* Author to whom correspondence should be addressed (ipuchtel@umd.edu).

† Present address: Isotope Geochemistry Laboratory, Department of Geology, University of Maryland, College Park, Maryland 20742 USA

‡ Present address: National High Magnetic Field Laboratory & Department of Geological Sciences, Florida State University, Tallahassee, Florida 32310 USA

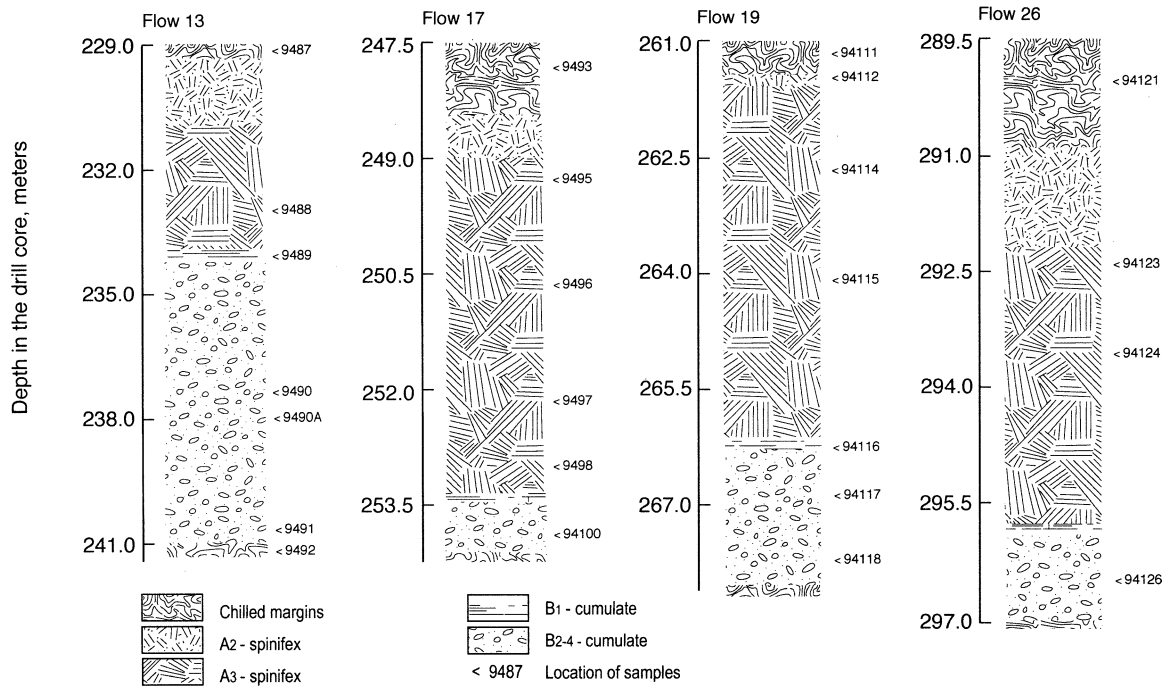


Fig. 1. Profiles through four differentiated komatiite lava flows at Kostomuksha that were sampled in detail. Note relatively thick spinifex zones and thin cumulate zones in all flows except for Flow 13. The thick flow top breccias point to a submarine eruption environment.

six samples from Flow 13, from which only one sample (9490) was previously analyzed. A much lower blank of the CT digestion procedure compared to the NiS fire-assay technique made it possible to obtain Re abundances. In this study, we have also obtained HSE abundances for a peridotite reference material UB-N, previously analyzed by high-pressure ashing (HPA) digestion ID-ICPMS technique (Meisel and Moser, 2004). On the basis of the new data, we revised values for the PGE compositions of the Kostomuksha emplaced komatiite lava, and for its mantle source. These data, when combined with the results for komatiites from the Abitibi greenstone belt (Puchtel et al., 2004b), provide new constraints on the possible nature of HSE abundances in mantle sources with both supra-chondritic and chondritic $^{187}\text{Os}/^{188}\text{Os}$ isotopic compositions.

2. GEOLOGICAL-GEOCHRONOLOGICAL BACKGROUND AND SAMPLING

The details of geology, petrology, and mineralogy, as well as trace element and Pb, Nd, and Os isotope systematics of mafic and ultramafic lavas from the Kostomuksha greenstone belt have been previously reported by Puchtel et al. (1998, 2001). The mafic terrane of the Kostomuksha synform is part of the Gimola-Kostomuksha greenstone belt in NW Karelia, Baltic Shield. The terrane contains submarine-erupted komatiite and basalt lavas, mafic and ultramafic volcanoclastic sediments, and numerous gabbro and peridotite sills. The komatiites and basalts have Sm-Nd and Pb-Pb whole rock isochron ages of 2843 ± 39 and 2813 ± 78 Ma, respectively. The whole sequence is intruded and overlain by mafic and felsic subvolcanic, volcanic, and volcanoclastic rocks with a U-Pb zircon age of 2821 ± 1 Ma (Puchtel et al., 1998). As a result of seafloor alteration

and/or greenschist facies metamorphism, the igneous mineralogy of the lavas was almost completely replaced by serpentine-chlorite-magnetite assemblages at 2757 ± 113 Ma (Puchtel et al., 1998). However, primary volcanic textures, structures, and most chemical features remained intact. For a selected set of komatiite samples and a chromite separate, Puchtel et al. (2001) obtained a Re-Os isochron corresponding to the age of 2795 ± 40 Ma and a radiogenic initial $\gamma^{187}\text{Os} = +3.6 \pm 1.0$. The lithophile trace element and isotope characteristics of the komatiites (e.g., $(\text{Nb}/\text{Th})_n = 1.5 - 2.1$, $\epsilon\text{Nd}(\text{T}) = +2.8 \pm 0.2$, $\mu_1 = 8.77 \pm 0.02$) resemble those of the contemporary oceanic mantle (Puchtel et al., 1998). On the basis of geological evidence and isotope and geochemical data, Puchtel et al. (1998) argued that the mafic terrane represented remnants of the upper crustal part of an Archean oceanic plateau derived from partial melting in a starting mantle plume head.

Twenty-seven drill core samples from seven differentiated komatiite lava flows have been analyzed in this study for PGEs and Re. Out of these, six new samples from Flow 13, for which major element data were not available, were also analyzed for major elements. Samples 9487–94126 (except for 94104) come from the four flows (13, 17, 19, and 26) shown in Figure 1. Samples 9469, 9479, and 94104 are from three other flows (#8, 10, and 18). The flows consist of an upper spinifex zone (A) and a lower cumulate zone (B). The spinifex zone contains an up to 1 m thick chilled margin at the top, which grades downward into a subzone of random, and then oriented, platy olivine spinifex. A distinct feature of all komatiite flows studied at Kostomuksha compared to those we examined at Alexo and Pyke Hill (Puchtel et al., 2004b) is a very small thickness of cumulate zones in the former, normally <20% of the total

Table 1. HSE data (ppb) for the UB-N peridotite standard.

Sample	T, °C	Time, h	Re	Os	Ir	Ru	Pt	Pd
UB-N (1)	240	24	0.188	3.16	2.91	6.15	7.23	6.05
UB-N (2)	240	48	0.255	4.41	3.51	8.45	8.09	6.00
UB-N (3)	240	96	0.186	3.67	3.54	7.38	7.43	6.35
UB-N (4)	270	24	0.187	4.03	4.10	7.71	7.07	5.80
UB-N (5)	270	48	0.185	3.31	3.47	6.88	7.55	5.93
UB-N (6)	270	72	0.190	3.37	3.34	6.65	7.55	6.54
UB-N (7)	270	96	0.188	3.51	3.74	7.46	7.43	6.02
Average			0.197	3.64	3.52	7.24	7.48	6.10
$\pm 2\sigma_{\text{mean}}$			0.02 (10%)	0.33 (9%)	0.27 (8%)	0.57 (8%)	0.24 (3%)	0.19 (3%)
UB-N ¹			0.206	3.71	3.38	6.30	7.42	6.11
$\pm 2\sigma_{\text{mean}}$			0.01 (2%)	0.26 (7%)	0.22 (6%)	0.30 (5%)	0.30 (4%)	0.18 (3%)

Before digestion at 270°C, aliquots (4) to (7) were preheated at 240°C for 24 h.

¹ Data of Meisel and Moser (2004) obtained by the HPA digestion ID-ICPMS technique.

thickness of the flows. One exception is Flow 13, which is ~11 m thick and contains a ~7-m thick cumulate zone. Further details of geology, petrology, and mineralogy, as well as lithophile trace element and Pb, Nd, and Os isotope geochemistry of the lavas, can be found in Puchtel et al. (1998, 2001).

3. ANALYTICAL TECHNIQUES

3.1. Major and Minor Element Analysis

Major and minor (Cr, Ni) element abundances in the six whole rock samples from Flow 13, not previously reported by Puchtel et al. (1998), were determined on pressed powder pellets by wavelength-dispersive X-ray fluorescence spectrometry using a VRA-20R spectrometer at the Institute of Geology and Geophysics in Novosibirsk. The accuracy and reproducibility of the analyses were ~1% and ~3% (relative) for major and minor elements, respectively. Major element abundances in all other samples, reported in the Puchtel et al. (1998) study, and for the sake of completeness presented here, were also determined at the Institute of Geology and Geophysics in Novosibirsk using the same technique. The abundances of Cr and Ni in these samples were measured on fused glass disks by wavelength-dispersive X-ray fluorescence spectrometry using an automated Philips PW-1404 spectrometer at the Johannes-Gutenberg-Universität in Mainz, with an accuracy and reproducibility of ~1% (relative).

3.2. HSE Analysis

In this study, we used a mixed komatiite spike #000531, also utilized by Puchtel et al. (2004a, 2004b) in their study of Abitibi komatiites. By contrast, the multielement spike used by Puchtel and Humayun (2000) had been optimized for primitive mantle abundances.

PGE and Re abundances were determined at The University of Chicago using a Carius tube digestion ID-ICPMS technique (Puchtel and Humayun, 2001; Puchtel et al., 2004a, 2004b). We used aliquots of the same batches of rock powders utilized by Puchtel and Humayun (2000). Samples were digested in 25 mL Pyrex borosilicate glass Carius tubes at 270°C for 48 h or at 240°C for 72 h after preheating at 240°C for 24 h. Osmium was extracted from the aqua regia sample solutions using the CCl₄ solvent extraction technique (Cohen and Waters, 1996), and then back-extracted into HBr, followed by purification via microdistillation (Birck et al., 1997). A 50% aliquot of the residual aqua regia solution was dried, converted into chloride form, taken up in 0.15N HCl, and Ir, Ru, Pt, Pd, and Re were separated from the matrix and further double purified by cation exchange chromatography. The resulting eluate was used directly for ICPMS analysis.

Measurements of Os, Ir, Ru, Pt, Pd, and Re isotopic compositions were performed on a Finnigan Element single-collector, magnetic sector, high-resolution ICPMS. The sample solutions were introduced into the ICPMS torch via a CETAC MCN6000 desolvating nebulizer for the PGE measurements, or via an ESI low-flow nebulizer with ESI Teflon spray chamber for the Re measurements. Typical count rates

were 10⁵–10⁶ cps for PGEs and 10⁴–10⁵ cps for Re, and the internal precisions of individual runs were better than 0.5% relative ($2\sigma_{\text{mean}}$). Long-term reproducibilities of a 0.5 ppb in-house Ir-Ru-Pd-Pt-Re standard solution and a 1 ppb Os standard solution, which characterize the external precision of the analysis, were ~1% ($2\sigma_{\text{stdev}}$) on all isotope ratios. Isobaric interferences of ¹⁰²Pd on ¹⁰²Ru and of ¹⁹⁸Hg on ¹⁹⁸Pt were corrected, and those from Mo, NiAr⁺, and Cd were monitored at masses 95, 98, and 111. These corrections were normally <0.5%. Mass fractionation for Ru, Pd, Ir, Pt, and Re was corrected using ⁹⁹Ru/¹⁰²Ru = 0.4044, ¹¹⁰Pd/¹⁰⁶Pd = 0.4288, ¹⁹¹Ir/¹⁹³Ir = 0.5942, ¹⁹⁸Pt/¹⁹⁵Pt = 0.2130, and ¹⁸⁵Re/¹⁸⁷Re = 0.5974 relative to those measured in the standard solution that was run alternately with samples. The measured ¹⁹⁰Os/¹⁹²Os ratios in the samples were corrected for fractionation using a linear law and ¹⁹²Os/¹⁸⁸Os = 3.083. The total analytical blank was 5 pg Os, 0.5 pg Ir, 3 pg Ru, 31 pg Pt, 7 pg Pd, and 10 pg Re. Blank corrections applied were <0.1% for Os, Ir, Ru, and Pd, ~0.3% for Pt, and <1.5% for Re.

Establishing the accuracy of PGE analysis is an unresolved issue in the analytical community (Meisel and Moser, 2004). For interlaboratory comparison of data reported from this lab, Puchtel et al. (2004b) carried out replicate analyses of HSE in komatiite standard KAL-1 and peridotite standard GP-13. The average PGE concentrations in KAL-1 measured by Puchtel et al. (2004b) are within 1 to 8% of both our previous estimates (Puchtel and Humayun, 2000) and the data of Rehkämper et al. (1999b). The average PGE abundances in GP-13 obtained by Puchtel et al. (2004b) are within 1 to 9% of those reported at Durham University, Leoben University, and the Danish Lithosphere Center using the ID-ICPMS method and both Carius tube and high-pressure ashing (HPA) digestion techniques (see review by Pearson et al., 2004).

Recently, Meisel and Moser (2004) presented HPA digestion ID-ICPMS analyses of Re and PGEs in the serpentinite reference material UB-N, and compared those with analyses obtained by Carius tube digestions to conclude that the latter technique was less efficient in extracting PGEs, especially Os, Ir, and Ru. To test this, we performed a time-temperature series of digestions of seven powder aliquots of serpentinite reference material UB-N using the analytical techniques applied here. The rationale behind this experiment was that if a refractory phase in UB-N was only partially dissolved by Carius tube digestion, then increasing the temperature or the run duration should increase the yield of Os, Ir, and Ru extraction. Obtaining a plateau in such a series would indicate quantitative digestion of that phase. The results of this experiment are reported in Table 1. The reproducibility was 3 to 10%, and no time dependence was observed for digestions that lasted from 24 to 96 h at temperatures of 240°C and 270°C. For the UB-N standard, the mean Re, Os, Ir, Pt, and Pd abundances obtained here are within 1 to 4% of those reported by Meisel and Moser (2004), whereas our Ru abundances are ~15% higher. Thus, this experiment has indicated that the Carius tube digestion method is at least as efficient in dissolving PGE carriers in serpentinitized peridotitic materials as the HPA digestion technique.

Table 2. Major (in wt%) and minor (in ppm) element data for Kostomuksha komatiites.

Depth, m	SiO ₂	TiO ₂	Al ₂ O ₃	Fe ₂ O ₃	MnO	MgO	CaO	Na ₂ O	K ₂ O	P ₂ O ₅	LOI	Cr	Ni	
Flow 8 (197.5–201.0)														
9469	197.7	44.0	0.502	8.43	14.2	0.17	25.8	6.90	0.01	0.02	0.07	6.49	3127	1138
Flow 10 (224.0–225.5)														
9479	224.8	44.6	0.430	7.31	13.0	0.17	27.8	6.55	0.01	0.02	0.07	7.05	3083	1232
Flow 13 (229.0–241.1)														
9487	229.2	46.1	0.426	7.03	11.2	0.19	27.9	7.03	0.00	0.01	0.15	6.66	3097	1371
9488	233.0	46.7	0.495	8.50	12.4	0.18	24.2	7.38	0.00	0.02	0.18	5.27	3314	1108
9489	234.2	44.6	0.393	6.70	10.2	0.18	29.2	8.56	0.00	0.01	0.21	8.66	3027	1497
9490	237.3	43.4	0.261	4.48	11.0	0.17	37.3	3.32	0.01	0.01	0.03	11.6	2466	2119
9490A	238.1	44.2	0.264	4.53	10.5	0.18	37.1	3.08	0.11	0.01	0.08	11.0	2409	2077
9491	240.7	44.1	0.327	5.58	10.9	0.18	32.3	6.47	0.00	0.01	0.16	7.73	2703	1688
9492	241.1	46.4	0.445	7.65	11.5	0.17	26.4	7.17	0.00	0.02	0.16	5.75	3191	1274
Flow 17 (247.5–254.0)														
9493	247.9	44.7	0.459	7.91	13.2	0.17	26.4	6.98	0.09	0.02	0.06	6.27	3120	1244
9495	249.3	44.4	0.469	7.55	13.4	0.17	26.6	7.32	0.02	0.03	0.07	5.93	3096	1325
9496	250.7	45.0	0.489	7.89	13.8	0.18	25.4	7.12	0.01	0.02	0.07	5.65	2968	1103
9497	252.2	45.6	0.476	7.75	13.7	0.18	24.8	7.37	0.01	0.03	0.06	5.19	3022	1147
9498	253.0	44.8	0.509	8.47	13.4	0.18	24.1	7.97	0.22	0.03	0.06	5.70	3244	1097
94100	253.9	43.7	0.290	5.19	11.2	0.21	34.8	4.49	0.01	0.02	0.06	10.1	2612	1889
Flow 18 (254.0–261.0)														
94104	257.0	45.3	0.412	7.12	12.2	0.18	27.9	6.77	0.01	0.02	0.05	7.69	2946	1378
Flow 19 (261.0–268.0)														
94111	261.2	46.2	0.416	7.15	11.7	0.16	27.4	6.95	0.04	0.02	0.08	6.39	3009	1401
94112	261.5	45.5	0.437	7.39	12.8	0.16	26.7	6.73	0.16	0.02	0.06	6.06	3040	1327
94114	262.6	45.5	0.398	6.97	12.2	0.17	28.3	6.31	0.01	0.02	0.07	7.21	2895	1456
94115	264.0	45.6	0.448	7.18	12.9	0.18	26.2	7.37	0.01	0.02	0.06	6.43	3084	1305
94116	266.3	45.0	0.319	5.41	11.4	0.19	32.7	4.98	0.01	0.02	0.06	9.02	2743	1797
94117	266.9	42.6	0.210	3.56	10.3	0.17	40.2	2.98	0.01	0.01	0.02	14.0	2273	2413
94118	267.7	43.6	0.241	4.17	11.2	0.19	37.1	3.38	0.01	0.01	0.04	10.9	2430	2145
Flow 26 (289.5–297.0)														
94121	290.0	44.9	0.418	7.17	11.5	0.18	28.7	6.73	0.30	0.02	0.07	6.72	3151	1352
94123	292.3	44.7	0.500	8.12	13.6	0.17	25.5	7.14	0.16	0.03	0.06	6.11	3250	1175
94124	293.5	45.7	0.467	7.79	13.0	0.18	24.9	7.80	0.14	0.03	0.07	5.50	3109	1104
94126	296.5	44.2	0.300	5.07	11.6	0.19	33.6	4.94	0.01	0.01	0.05	9.90	2763	1861

Analyses recalculated on an anhydrous basis.

4. RESULTS

4.1. Major and Minor Element Data and the MgO Content of the Emplaced Komatiite Lava

Major and minor (Cr, Ni) element data for all samples analyzed for HSE in this study are presented in Table 2, and the abundances of Al, Ti, Cr, and Ni are plotted against MgO on the variation diagrams in Figure 2. Samples from Flow 13, including two chilled margin samples, plot on the same olivine fractionation trends as samples from the other flows, and thus, show no evidence of postmagmatic disturbance of these elements, as concluded by Puchtel et al. (1998). The average MgO content of the chilled margin samples from the four complete lava flows studied is $27.4 \pm 0.4\%$ and is considered here to reflect the MgO content of the emplaced komatiite lavas. This value is identical to $27 \pm 1\%$ MgO calculated by Puchtel et al. (1998) for a larger number of komatiite lava flows using several independent approaches.

Both compatible (MgO, Ni) and incompatible elements (Al, Ti, Cr) exhibit variations across the lava flows, typical of those reported for other differentiated komatiite lava units worldwide with a comparable MgO content (e.g., see recent review by Puchtel et al., 2004b). The MgO content varies between 24 and 28% in the A zone, generally decreasing towards the lowermost part of it, and between 29 and 40% in the B zone. The highest

MgO content (40%) is observed in the cumulate portion of Flow 19, whereas in the cumulate zone of Flow 13, the MgO content does not exceed $\sim 37\%$.

4.2. PGE and Re Abundances in the Emplaced Komatiite Lava

PGE and Re data for the analyzed samples are listed in Table 3 and are plotted on the variation diagrams in Figure 3. PGE data are also plotted as CI chondrite-normalized abundances in Figure 4. The PGE abundances in the emplaced komatiite lava were calculated from an average PGE content of the chilled margin samples, which have been shown to represent the composition of the emplaced komatiite lava at Kostomuksha (Puchtel et al., 1998). These samples plot on the bulk differentiation trends for PGEs (Fig. 3) and do not show any evidence of postmagmatic PGE mobility. Nine analyses of five samples indicate that the emplaced komatiite lava contained 1.9 ppb Os and was characterized by a slightly supra-chondritic $(\text{Os}/\text{Ir})_{\text{N}} = 1.07$ and a moderately fractionated PGE pattern with $(\text{Pd}/\text{Ir})_{\text{N}} = 5.2$ (Table 3; Fig. 4).

Unlike PGEs, the Re abundances display a totally irregular behavior on the MgO vs. Re plot due to a Re mobility during seafloor alteration and/or subsequent greenschist facies metamorphism, as was also concluded by Puchtel et al. (2001). This

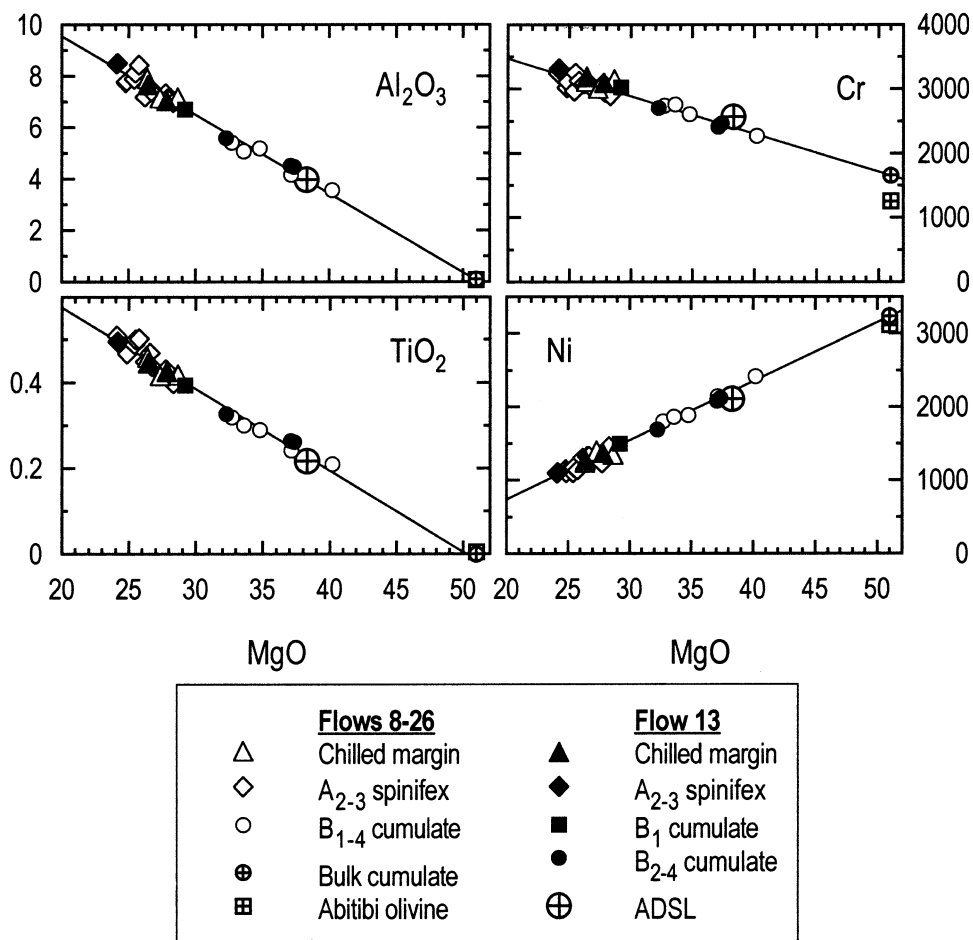


Fig. 2. Variation diagrams of Al, Ti (wt%), and Cr and Ni (ppm) vs. MgO (wt%) for Kostomuksha komatiites. The composition of Abitibi olivine was adopted from Puchtel et al. (2004b). The trends represent best fit lines drawn through the komatiite analytical data points. Note that the trends pass through or close to the olivine compositions and thus represent olivine control lines. The bulk cumulate was calculated from the differentiation trends assuming that its MgO abundance was determined by that of olivine (i.e., was equal to 51%). Average depleted spinel lherzolite (ADSL) from Puchtel et al. (2004b).

makes it impossible to estimate the Re content of the emplaced komatiite lava with any degree of confidence.

4.3. Comparison of PGE and Re Abundances Obtained by Different Methods

To compare the results obtained using two different digestion techniques, also presented in Figure 3 and Table 3 are PGE data from the Puchtel and Humayun (2000) study. The abundances of Os, Ir, and Pt in the emplaced komatiite lava obtained here are, on average, 22 to 25% higher, and abundances of Ru are ~34% higher, compared to those reported by Puchtel and Humayun (2000). We attribute the discrepancies between the results from the NiS fire-assay and Carius tube digestion techniques to incomplete dissolution of PGE carriers, mostly chromite, during the NiS fire-assay procedure. A similar interpretation has been put forward by Puchtel et al. (2004b), who have digested a large set of samples of Abitibi komatiites using both the Carius tube and NiS fire-assay techniques. In their study, the observed discrepancies between the results from the two digestion techniques were even larger, likely

due to a better state of preservation of mineral phases in the Abitibi samples. The Pd contents are identical between the two techniques, indicating that Pd is not hosted by a phase that is resistant in the NiS fire-assay digestion procedure.

4.4. PGE Fractionation During Magmatic Differentiation

In the variation diagrams (Fig. 3), Pt and Pd abundances in all samples show a strong ($r = 0.97-0.98$) inverse correlation with MgO, indicating that these PGEs behaved incompatibly during lava differentiation. The bulk $D_{Pt, Pd}^{Sol-Liq}$ of <0.1 was calculated from the MgO vs. Pt and Pd differentiation trends in Figure 3, using the MgO content of the emplaced komatiite lava of ~27% and assuming that the MgO content of the bulk cumulate was determined by olivine and was ~51% (Puchtel et al., 1998). The bulk $D_{Pt}^{Sol-Liq}$ from this study (0.09) is much lower than that obtained by Puchtel and Humayun (2000) (0.52), whereas $D_{Pd}^{Sol-Liq}$ is similar.

According to the IPGE (IPGEs: Os, Ir, and Ru; Barnes et al., 1985) behavior during lava differentiation, all lava flows ana-

Table 3. PGE and Re abundances (in ppb) in Kostomuksha komatiites.

Sample	Re	Os	Ir	Ru	Pt	Pd	(Os/Ir) _N	(Pd/Ir) _N	Pt/Ti	Pd/Pt
9469		1.75	1.65	5.69	10.7	11.5	1.05	5.99	3.57	1.07
9469		<i>1.53</i>	<i>1.59</i>	<i>3.97</i>	<i>9.19</i>	<i>12.0</i>	<i>0.95</i>	<i>6.48</i>	<i>3.05</i>	<i>1.31</i>
9479	0.939	2.01	1.88	5.59	10.5	11.0	1.06	5.03	4.05	1.05
9479		<i>1.77</i>	<i>1.71</i>	<i>4.04</i>	<i>8.51</i>	<i>11.2</i>	<i>1.03</i>	<i>5.62</i>	<i>3.30</i>	<i>1.31</i>
9487	0.684	1.83	1.70	5.84	10.5	11.0	1.06	5.55	4.13	1.04
9488	0.559	0.742	0.878	5.60	11.6	11.5	0.84	11.3	3.92	0.99
9489	2.44	0.774	0.889	5.92	9.78	8.80	0.86	8.50	4.16	0.90
9490*	0.040	5.11	4.15	5.75	6.24	4.97	1.22	1.03	3.99	0.80
9490*	0.045	5.26	4.26	5.87	7.12	6.60	1.22	1.33	4.56	0.93
9490		<i>6.19</i>	<i>6.15</i>	<i>4.93</i>	<i>6.82</i>	<i>5.37</i>	<i>1.00</i>	<i>0.75</i>	<i>4.36</i>	<i>0.79</i>
9490A	0.051	4.55	3.79	5.95	6.84	5.95	1.19	1.35	4.32	0.87
9491	0.739	2.94	2.47	5.93	8.03	8.26	1.18	2.88	4.10	1.03
9492	0.540	1.87	1.69	5.86	10.9	11.0	1.09	5.57	4.07	1.01
9493*		2.02	1.85	5.98	11.3	10.7	1.08	4.98	4.12	0.95
9493*	0.546	1.96	1.77	5.93	11.3	10.1	1.10	4.90	4.10	0.90
9493*	0.604	2.22	1.98	5.97	11.0	9.87	1.11	4.27	4.00	0.90
9493		<i>1.50</i>	<i>1.39</i>	<i>4.31</i>	<i>9.13</i>	<i>11.1</i>	<i>1.04</i>	<i>6.40</i>	<i>2.96</i>	<i>1.28</i>
9495	0.749	1.94	1.62	5.89	10.6	10.3	1.18	5.45	3.76	0.97
9495		<i>1.29</i>	<i>1.27</i>	<i>3.77</i>	<i>8.62</i>	<i>10.6</i>	<i>1.01</i>	<i>7.20</i>	<i>2.83</i>	<i>1.23</i>
9496	0.145	1.85	1.60	5.64	10.5	10.5	1.14	5.63	3.59	0.99
9496		<i>1.53</i>	<i>1.53</i>	<i>3.69</i>	<i>8.62</i>	<i>11.2</i>	<i>0.99</i>	<i>6.33</i>	<i>2.94</i>	<i>1.30</i>
9497	0.183	1.86	1.66	5.69	11.4	11.0	1.11	5.68	3.99	0.97
9497		<i>1.43</i>	<i>1.51</i>	<i>3.83</i>	<i>8.38</i>	<i>11.7</i>	<i>0.94</i>	<i>6.68</i>	<i>2.94</i>	<i>1.40</i>
9498	0.123	1.95	1.72	5.72	11.3	11.3	1.13	5.67	3.71	1.00
9498		<i>1.50</i>	<i>1.61</i>	<i>3.90</i>	<i>8.27</i>	<i>11.4</i>	<i>0.92</i>	<i>6.05</i>	<i>2.71</i>	<i>1.37</i>
94100*			1.20	5.27	7.56	6.38		4.56	4.35	0.84
94100*		1.47	1.28	5.13	7.41	6.05	1.14	4.08	4.26	0.82
94100*	0.100	1.50	1.34	5.45	7.34	6.94	1.11	4.43	4.23	0.94
94100		<i>1.19</i>	<i>1.26</i>	<i>4.19</i>	<i>7.37</i>	<i>5.92</i>	<i>0.95</i>	<i>4.15</i>	<i>4.18</i>	<i>0.83</i>
94104	0.546	1.73	1.64	5.73	10.5	10.6	1.05	5.56	4.27	1.01
94104		<i>1.56</i>	<i>1.46</i>	<i>3.79</i>	<i>8.11</i>	<i>9.97</i>	<i>1.06</i>	<i>5.87</i>	<i>3.29</i>	<i>1.23</i>
94111*		1.71	1.67	5.65	10.3	11.0	1.01	5.65	4.15	1.06
94111*	0.895	1.89	1.76	5.82	10.4	10.7	1.06	5.22	4.17	1.03
94111*	0.920	1.81	1.67	5.76	10.2	10.4	1.08	5.37	4.10	1.02
94111		<i>1.55</i>	<i>1.42</i>	<i>4.36</i>	<i>8.64</i>	<i>11.5</i>	<i>1.03</i>	<i>6.76</i>	<i>3.14</i>	<i>1.39</i>
94112	0.574	1.78	1.53	5.56	9.79	10.4	1.15	5.81	3.74	1.06
94114	0.711	1.75	1.54	5.59	9.56	9.45	1.12	5.25	4.01	0.99
94114		<i>1.38</i>	<i>1.33</i>	<i>3.67</i>	<i>7.78</i>	<i>9.60</i>	<i>1.00</i>	<i>6.23</i>	<i>3.26</i>	<i>1.24</i>
94115	0.508	1.90	1.68	5.62	10.4	11.1	1.12	5.70	3.86	1.07
94116		1.58	1.43	5.41	7.44	7.51	1.09	4.50	3.89	1.01
94116		<i>1.40</i>	<i>1.37</i>	<i>3.94</i>	<i>7.66</i>	<i>7.48</i>	<i>1.01</i>	<i>4.79</i>	<i>4.01</i>	<i>0.99</i>
94117		1.24	1.18	5.22	5.20	4.90	1.04	3.56	4.14	0.94
94117		<i>1.16</i>	<i>1.20</i>	<i>4.01</i>	<i>5.89</i>	<i>5.11</i>	<i>0.95</i>	<i>3.65</i>	<i>4.68</i>	<i>0.87</i>
94118		1.32	1.15	5.27	6.37	5.98	1.13	4.45	4.41	0.94
94118		<i>1.37</i>	<i>1.28</i>	<i>3.80</i>	<i>6.20</i>	<i>6.05</i>	<i>1.05</i>	<i>4.05</i>	<i>4.29</i>	<i>0.98</i>
94121	0.278	1.86	1.74	5.68	10.4	10.5	1.06	5.20	4.16	1.01
94121		<i>1.40</i>	<i>1.33</i>	<i>3.40</i>	<i>9.42</i>	<i>10.2</i>	<i>1.04</i>	<i>6.61</i>	<i>3.40</i>	<i>1.20</i>
94123	0.275	2.01	1.77	6.00	11.5	11.0	1.13	5.35	3.85	0.96
94123		<i>1.52</i>	<i>1.47</i>	<i>3.40</i>	<i>9.42</i>	<i>11.4</i>	<i>1.02</i>	<i>6.69</i>	<i>3.15</i>	<i>1.21</i>
94124	0.398	2.01	1.71	5.69	11.3	11.0	1.16	5.52	4.04	0.97
94126*			1.43	5.35	7.47	6.67		4.02	4.16	0.89
94126*		1.64	1.41	5.41	7.23	7.36	1.15	4.49	4.02	1.02
94126*	0.119	1.56	1.42	5.51	7.81	7.46	1.09	4.52	4.35	0.95
94126		<i>1.43</i>	<i>1.54</i>	<i>3.53</i>	<i>7.63</i>	<i>6.64</i>	<i>0.93</i>	<i>3.77</i>	<i>4.17</i>	<i>0.89</i>

Normalizing values (N) from Anders and Grevesse (1989). Plain text and boldfaced values (this study) samples digested at 240°C and 270°C for 48–72 h, respectively; italicized values - data from Puchtel and Humayun (2000).

* Separate CT digestions of aliquots from the same batches of sample powder.

lyzed in this study were subdivided into two types. Samples from the first, dominant type, which we term the Kostomuksha type, in the MgO vs. Os, Ir, and Ru diagrams plot on the trend lines with negative slopes indicating an incompatible behavior. In this type of lavas, spinifex-textured samples with the lowest MgO content have the highest PGE abundances (Fig. 4). This was the only type recognized in the Puchtel and Humayun

(2000) study. The bulk $D^{\text{Sol-Liq}}$ calculated in this study are 0.37, 0.41, and 0.81 for Os, Ir, and Ru, respectively. The bulk $D_{\text{Os, Ir}}^{\text{Sol-Liq}}$ are two times lower than those obtained by Puchtel and Humayun (2000) for this type of lavas (0.70 and 0.75). Also plotted in Figure 3 are average PGE and Re abundances in olivine from Abitibi komatiites (Puchtel et al., 2004b), which have compositions of emplaced lava similar to that at Kosto-

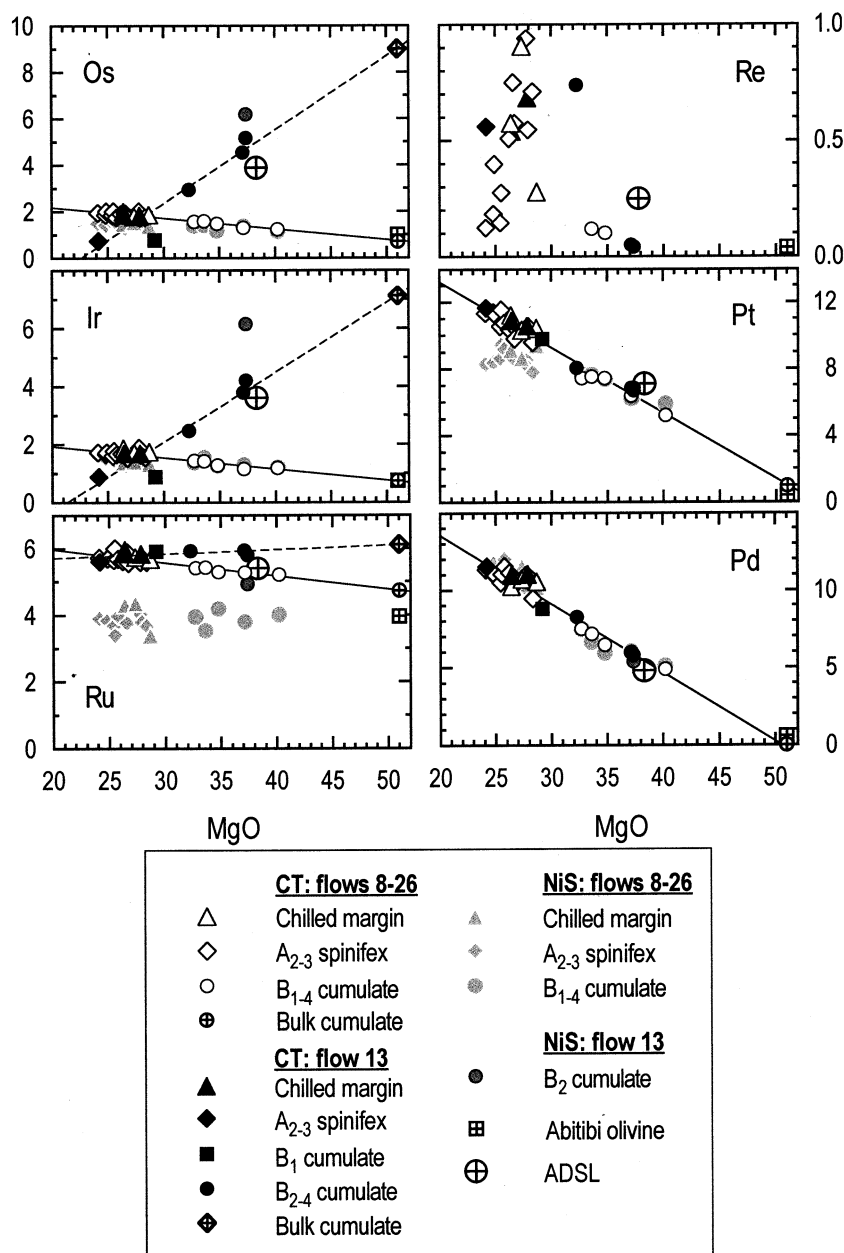


Fig. 3. Variation diagrams of HSE (ppb) vs. MgO (wt%) for Kostomuksha komatiites. The trends represent best fit lines drawn through the komatiite analytical data points. Note that the IPGE data for samples from Flow 13 plot on trends (dashed lines) with positive slopes, indicating compatible (Munro type) behavior during lava differentiation, whereas the IPGE data for the other flows plot on trends (solid lines) with negative slopes, indicating an incompatible (Kostomuksha type) behavior during lava differentiation. The latter trends also pass through or close to the composition of Abitibi olivine. Platinum and Pd data for both Kostomuksha- and Munro-type komatiites plot on the olivine control lines, and the calculated compositions of bulk cumulates are similar to that of olivine. Rhenium data exhibit a totally irregular behavior as a result of Re mobility during postmagmatic processes. The data from Puchtel and Humayun (2000) obtained by the NiS fire-assay ID-ICPMS technique are shown for comparison. See also legend for Figure 2 and text for explanation.

muksha. The olivine composition plots on or close to the regression lines for all PGEs except Ru, thus confirming the conclusion of Puchtel and Humayun (2000) that PGE variations in this type of lava were controlled by a single phase, olivine.

In contrast to the Kostomuksha-type flows, Os, Ir, and Ru data for samples from the second type, represented by Flow 13 and which we term the Munro type, plot along trends with

positive slopes, indicating a compatible behavior during lava differentiation. In this type of lava, spinifex-textured samples and B₁ cumulates have the lowest IPGE content, and B₂₋₄ cumulates have the highest IPGE abundances (Fig. 4). This is something that was not completely realized by Puchtel and Humayun (2000), who at that time analyzed only one cumulate sample from this flow (9490). This type of compatible behav-

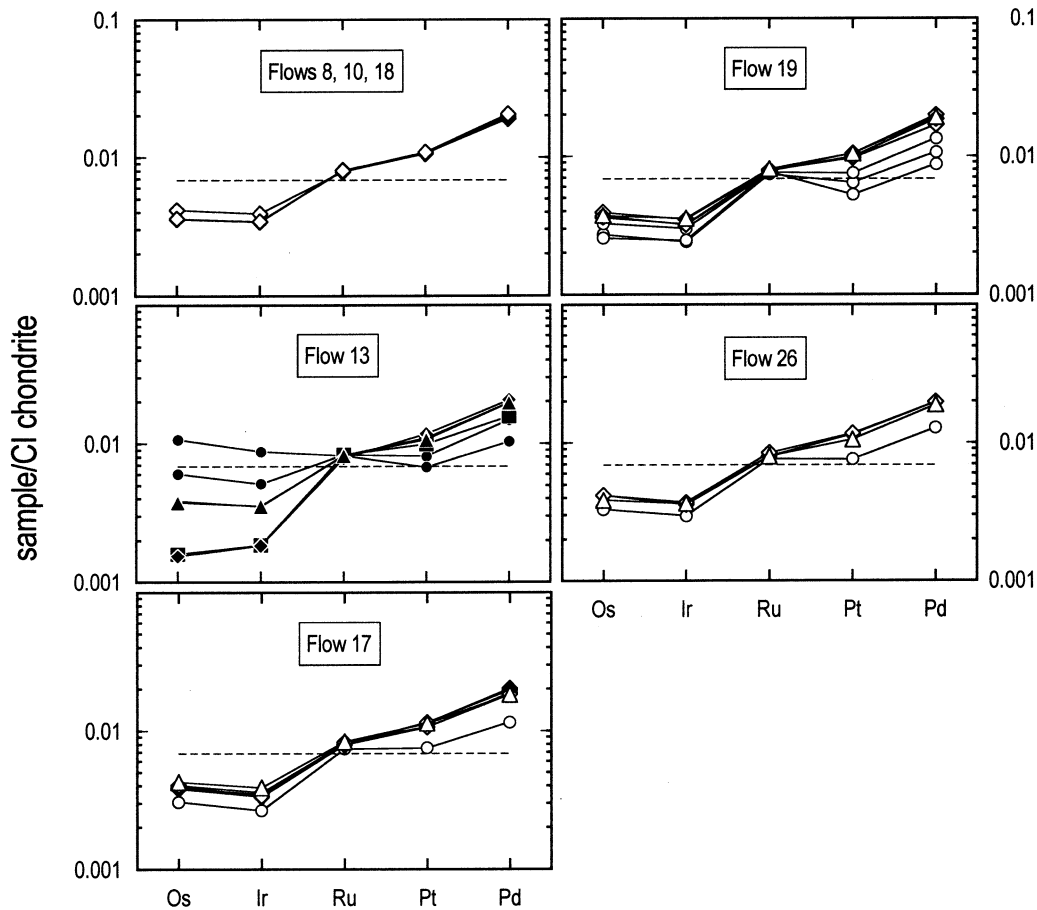


Fig. 4. CI chondrite-normalized (Anders and Grevesse 1989) PGE abundances in Kostomuksha komatiites. Triangles = chilled margins; diamonds = A_{2-3} spinifex; squares = B_1 cumulate; and circles = B_{2-4} cumulates. Composition of the primitive upper mantle (dashed line) is calculated assuming an Ir content of 3.3 ppb (Morgan, 1986) and CI chondrite relative abundances of Anders and Grevesse (1989).

ior, with the bulk $D^{Sol-Liq}$ of 4.8, 4.1, and 1.1 for Os, Ir, and Ru, respectively, is similar to that found in Pyke Hill and Alexo komatiites (Puchtel et al., 2004b).

5. DISCUSSION

5.1. Thickness of Cumulate Zone and IPGE Behavior During Lava Differentiation

The Kostomuksha-type komatiite lavas are quite unique in their IPGE fractionation pattern as a function of lava differentiation. Indeed, many previous studies have demonstrated a strong positive correlation between Os, Ir, and MgO in lavas in which olivine was shown to be the major liquidus phase (Barnes et al., 1985; Crocket and MacRae, 1986; Brüggmann et al., 1987; Zhou, 1994; Barnes et al., 1995; Keays, 1995; Leshner and Stone, 1996; Rehkämper et al., 1999b; Puchtel and Humayun, 2001; Puchtel et al., 2004b). At the same time, it becomes increasingly clear that olivine alone played only a minor role in controlling the IPGE budget of mantle derived rocks. In their study of Alexo and Pyke Hill komatiites, Puchtel et al. (2004b) have established that there was a minor IPGE-rich phase present on the liquidus of the differentiated lava flows studied, which fractionated separately from olivine and concentrated

mostly in the lowermost cumulate part of the flows. However, the identity of this phase, and whether it was already present in the lava upon eruption or crystallized after emplacement, could not be established conclusively. In contrast, the IPGEs were incompatible during differentiation of the majority of komatiite lavas at Kostomuksha. The only other example known to the authors, where IPGEs are characterized by a similarly incompatible behavior, are komatiites from the Komati formation in the Barberton Mountain Land (Maier et al., 2003), although these komatiites have relatively low PGE abundances overall. One feature that distinguishes the Kostomuksha-type flows is very small thicknesses of cumulate zones, which constitute <20% of the total thicknesses of the flows. The only exception is Flow 13, in which cumulate zone occupies 2/3 of its thickness, and this flow does display the commonly observed Munro-type positive correlation between IPGEs and MgO.

Komatiite lava flows with thick spinifex zone and thin cumulate zone are less common than their counterparts, which are either massive throughout or contain a thick cumulate zone. The extent to which a spinifex zone is developed in any particular lava flow depends on the initial concentration of olivine phenocrysts, the temperature of the lava upon emplacement, and the thickness of the lava unit (Pyke et al., 1973;

Table 4. Results of modeling.

Sample	Os	Ir	Ru	Pt	Pd	MgO	TiO ₂	Al ₂ O ₃
Composition of emplaced komatiite lava at Kostomuksha								
[1]	1.90	1.75	5.81	10.7	10.6	27.4	0.432	7.39
[2]	1.45	1.38	3.86	8.22	10.6	27.5	0.431	7.41
Komatiite lava differentiation: calculated solid-liquid partition coefficients								
Bulk D1	0.38	0.42	0.81	0.09	<0.01	1.9	<0.01	0.03
Bulk D2	4.8	4.1	1.1	0.09	<0.01	1.9	<0.01	0.03
Olivine	0.43	0.35	0.70	0.04	0.05	1.9	0.01	0.01
Composition of mantle sources								
[3]	4.3	3.9	5.8	6.0	5.4	38.3	0.23	4.0
[4]	2.5	2.5	3.7	5.1	2.9	37.8	0.18	4.1
[5]	3.9	3.6	5.4	5.7	5.7	38.3	0.19	4.1
[6]	3.9	3.6	5.4	7.1	4.8	38.3	0.22	4.0

The bulk $D_{\text{PGE}}^{\text{Sol-Liq}}$ were calculated from the bulk differentiation trends in Fig. 3 assuming an MgO content of the bulk cumulate of 51% (i.e., its MgO content was determined by that of olivine) and using the PGE abundances in the emplaced lava [1]. Bulk D1 and D2 for IPGEs were calculated from data for the Kostomuksha- and Munro-type lavas, respectively; bulk Ds for Pt and Pd were calculated using data for both types of lavas.

$D^{\text{Ol-Liq}}$ are from Puchtel et al. (2004b). These apparent Ds were calculated using the average measured composition of Abitibi olivine and the average composition of the emplaced komatiite lava from which this olivine has crystallized.

[1] PGE data from this study; major element data from Puchtel et al. (1998).

[2] Data from Puchtel and Humayun (2000).

[3] Calculated source for Kostomuksha komatiites from this study.

[4] Calculated source for Kostomuksha komatiites from Puchtel and Humayun (2000).

[5] Calculated source for Abitibi komatiites from Puchtel et al. (2004a, 2004b).

[6] Average depleted spinel lherzolite, ADSL (Puchtel et al., 2004b).

Arndt et al., 1977). Where these factors combine to contribute to slow cooling, the lava remained liquid longer, and settling of liquidus phases occurred more efficiently, giving rise to a thicker spinifex zone. This implies that in flows with thick spinifex zones, the conditions for effective crystal settling were more favorable and thus, if the IPGE-rich phase was present in the lava upon eruption or had crystallized during lava cooling, it would have a better chance to accumulate in the lower part of the flow. Obviously, it did not happen in the Kostomuksha-type flows. Because there is no reason to believe that the Munro-type flows were more saturated with the IPGE-rich phase than the Kostomuksha-type, as both have the same PGE composition of the emplaced lava and were emplaced as consecutive flows, we conclude that in the Kostomuksha-type flows with a thin cumulate zone, settling of this phase was inhibited, whereas in the Munro-type lavas with a thick cumulate zone, this phase was settling freely. The cause for such a difference remains unclear, however.

5.2. PGE Composition of the Kostomuksha Mantle Source

The radiogenic $^{187}\text{Os}/^{188}\text{Os}$ isotopic composition of the Kostomuksha komatiite source established by Puchtel et al. (2001) indicates that, whatever its origin, this source evolved with a time-integrated supra-chondritic Re/Os ratio. Here, we determine the PGE abundances in the source of the Kostomuksha komatiites at the time of komatiite formation. These were calculated on the basis of several techniques and assumptions outlined in detail by Puchtel et al. (2004a, 2004b), which are only briefly summarized here. First, it was assumed that the abundances of moderately incompatible and compatible lithophile elements in the Kostomuksha source can be approximated by those in an average depleted spinel lherzolite (ADSL; Pu-

chtel et al., 2004b), as both are similarly depleted in large ion lithophile elements (LILE) such as LREE, Th, and U. As such, the degree of partial melting of the Kostomuksha source was calculated to be 48% using a batch partial melting model (Shaw, 1970), and the abundances of moderately incompatible elements (e.g., Al, Ti, Gd; $D^{\text{Sol-Liq}} < 0.1$; Green, 1994) in ADSL and in the Kostomuksha emplaced komatiite lava. At such high degrees of partial melting in the spinel to garnet peridotite stability field, all interstitial sulfide, which is the main host of Pt and Pd, is completely consumed (Barnes et al., 1985; Keays, 1995), and the only major phase that is left behind in the residue is olivine and possibly small amounts of majorite garnet (Arndt, 1976), as indicated by a slight depletion of heavy rare earth elements (HREE) in the Kostomuksha lavas (Puchtel et al., 1998). Hence, the abundances of moderately incompatible elements, including Pt and Pd, in the lava and in the source, must plot on olivine control lines in the MgO variation diagrams. Using 38.3% MgO in ADSL as an estimate of MgO abundance in the source of the Kostomuksha komatiite, from regressions in Figures 2 and 3, this source can be shown to contain 4.0% Al₂O₃, 0.23% TiO₂, 6.0 ppb Pt, and 5.4 ppb Pd. The calculated abundances of Al and Ti in the Kostomuksha komatiite source are identical to those in ADSL, whereas the Pt content is ~15% lower, and Pd content is ~10% higher in the Kostomuksha source compared to ADSL (Table 4).

The abundances of IPGEs that are compatible even during high degrees of partial melting cannot be calculated in the same manner as those of the incompatible elements, so a different approach was adopted here following the reasoning of Puchtel et al. (2004b). Ruthenium shows very little fractionation during komatiite lava differentiation, both at Kostomuksha and at Pyke Hill-Alexo. It is thus assumed that the bulk D_{Ru} was close to unity also during partial melting. The average Ru abundance in

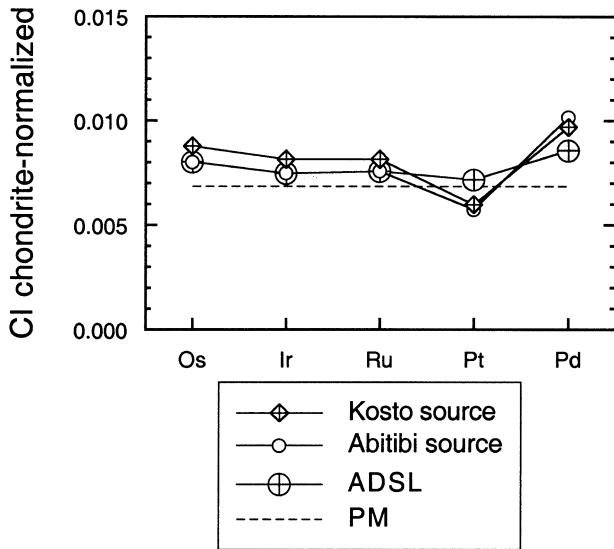


Fig. 5. CI chondrite-normalized (Anders and Grevesse, 1989) HSE abundances in the calculated source of the Kostomuksha komatiites. The PGE data for the source of Abitibi komatiites and for an average depleted spinel lherzolite (ADSL) from Puchtel et al. (2004b). Note the supra-chondritic Pd/Ir ratios in both sources and in ADSL.

the emplaced komatiite lavas is 5.8 ppb, so we assume that the Ru abundance in the komatiite source was also 5.8 ppb. This is slightly higher than that in ADSL (5.4 ppb) with an overall uncertainty of 2% ($2\sigma_{\text{mean}}$). The average $(\text{Os}/\text{Ir})_{\text{N}}$ ratio in the emplaced Kostomuksha komatiitic lava is close to CI-chondritic (1.07), is identical to that in the Abitibi emplaced komatiite lava (1.07), and is taken to be also such in the Kostomuksha mantle source, as Os/Ir ratios fractionate very little during partial melting. We assume that the Ru/Ir in the Kostomuksha source was CI-chondritic (1.48), which then yields the Os and Ir abundances in the source of 4.3 and 3.9 ppb, respectively (Table 4). These IPGE abundances are $\sim 10\%$ higher than those in ADSL and in the source of the Abitibi komatiites (Fig. 5).

Both the Kostomuksha and Abitibi sources are depleted in Pt and enriched in Pd with Pd/Pt of 0.90 and 1.0, respectively, thus revealing non-CI chondritic PGE patterns. This is a significant departure from the approach of Puchtel and Humayun (2000), who assumed a CI-chondritic source, and then assumed that “excess Pd” was present in the Kostomuksha emplaced lava due to melt-focusing of low-degree melt fractions from variable depths. It can be seen that there is no “excess” of Al, Ti, or Pt, which are equally incompatible during high degrees of partial melting, so that interpretation is abandoned here. The Pd/Pt ratio of the Kostomuksha komatiite source (0.90) is similar to that of the Abitibi komatiite source (1.00) obtained by Puchtel et al. (2004b), i.e., 60% higher than in a CI-chondritic mantle (0.57), indicating that “excess” Pd relative to a CI-chondrite mantle is a feature of komatiite mantle source regions which exhibit both radiogenic and chondritic long-term Re/Os ratios. Pattou et al. (1996) argued that the supra-chondritic Pd/Ir ratios observed in some upper mantle peridotites were evidence of a non-chondritic mantle PGE composition. However, Alard et al. (2000) observed high Pd/Ir- and low Pd/Ir-bearing sulfides by laser ablation ICPMS in the same set of xenoliths studied by Pattou et al. (1996) and argued that the

PGE patterns observed by these authors could be explained by the presence of these two sulfide phases in different proportions. Thus, supra-chondritic Pd/Ir ratios have been attributed to magmatic modifications of the upper mantle source regions of mantle xenoliths. Similarly, Rehkämper et al. (1999a) explained supra-chondritic Pd/Ir ratios of some abyssal peridotites in terms of melt percolation. Our results indicate that one must either accept that melt percolation has significantly enriched the Pd/Ir ratios of two independent komatiite source regions to almost exactly the same degree, or that such high Pd/Ir ratios are genuine characteristics of the Earth’s mantle.

Although the mantle sources of the Kostomuksha and Abitibi komatiites had very similar lithophile trace element, Pb- and Nd-isotope characteristics, and HSE compositions, they had distinct $^{187}\text{Os}/^{188}\text{Os}$ isotopic compositions. The source of the Kostomuksha komatiites had a radiogenic $^{187}\text{Os}/^{188}\text{Os}$ ratio (Puchtel et al., 2001), whereas the source of the Abitibi komatiites had a nearly chondritic $^{187}\text{Os}/^{188}\text{Os}$ ratio (Gangopadhyay and Walker, 2003; Puchtel et al., 2004a). Puchtel et al. (2001) proposed that the enriched $^{187}\text{Os}/^{188}\text{Os}$ signature in the Kostomuksha komatiites was derived from the outer core. If this was indeed the case, the results obtained in this study have an important bearing on our understanding of the core-mantle interaction mechanism. Walker et al. (1995) postulated that core-mantle exchange occurred by physical mixing of outer core material into mantle plume sources. Although this process should have substantially enriched mantle sources of the lavas in Os, the fact that such an enrichment was not observed was later explained by difficulties in deducing the exact abundances of Os in the mantle sources from those in lavas (Shirey and Walker, 1998). Puchtel and Humayun (2000) demonstrated the potential of PGE studies on komatiites for resolving these issues. They estimated that, to account for the Os isotopic enrichment in the Kostomuksha komatiites, the amount of core material required by the physical mixing model is on the order of 1%, but noted that physical addition of such amount of outer core material would have increased the PGE abundances in the Kostomuksha source by about an order of magnitude. They compared the abundances of PGEs in their estimate of the Kostomuksha komatiite source with those in the source of the Alexo komatiites derived from KAL-1 and concluded that there was no evidence of PGE addition to the Kostomuksha source.

Using the new PGE data for the Abitibi and Kostomuksha komatiites (Table 4), it is now possible to refine the conclusions of Puchtel and Humayun (2000) and to show that both sources contained essentially identical abundances of PGEs. This observation supports the conclusion of Puchtel and Humayun (2000) that if core-mantle interaction produced the supra-chondritic initial $^{187}\text{Os}/^{188}\text{Os}$ in the Kostomuksha komatiites, then some kind of isotopic exchange rather than physical mixing is required. Importantly, this conclusion is independent of any melting model. This means that the similarity in Ru contents of the Kostomuksha and Abitibi magmas can be used to compare PGE abundances in their respective mantle sources, and can then be applied to other komatiites to determine whether they were derived from mantle sources with enhanced PGE abundances.

6. SUMMARY AND CONCLUSIONS

1. PGE analysis by the Carius tube digestion ID-ICPMS technique produces data comparable to those obtained by the HPA digestion ID-ICPMS technique, provided Carius tubes are heated at $T \geq 240^\circ\text{C}$ for ≥ 48 h.
2. Incomplete digestion of chromite, and possibly some other PGE carriers, in samples of Kostomuksha komatiites during the NiS fire-assay procedure used by Puchtel and Humayun (2000) led to underestimation of Os, Ir, and Pt abundances by 22 to 25% and Ru abundances by 34% in the emplaced komatiite lava.
3. Two types of komatiite lavas have been distinguished in this study based on the IPGE behavior during lava differentiation. The first type, which we term the Kostomuksha-type, is characterized by an incompatible behavior of IPGEs during the lava differentiation. This type is quite unique, the only other known example being komatiites from the Komati Formation in the Barberton greenstone belt (Maier et al., 2003). The bulk partition coefficients for IPGEs calculated from the bulk differentiation trends in the Kostomuksha-type komatiite are similar to those for olivine. Cumulate zone in this type of komatiite lava occupies <20% of the total thickness of the flows. The second type, which we named the Munro type, exhibits a compatible behavior of IPGEs during the lava differentiation, with bulk partition coefficients similar to those obtained for Abitibi komatiites by Puchtel et al. (2004b). These bulk partition coefficients indicate that, as with the other Munro-type komatiite lavas, the bulk cumulate contained an IPGE-rich minor phase in addition to olivine. The cumulate zone in this type of komatiite occupies >20% of the total thickness of lava flows.
4. A non-CI chondritic PGE pattern has been established for the source of the Kostomuksha komatiites. This pattern is very similar to that calculated for Abitibi komatiites (Puchtel et al., 2004a, 2004b). The new results indicate that the non-CI chondritic HSE patterns are a genuine characteristic of the Earth's mantle.
5. The absolute PGE abundances in the source of the Kostomuksha komatiites are calculated to be identical to those in the source of the Abitibi komatiites to within $\sim 10\%$.
6. The conclusion of Puchtel and Humayun (2000) that core-mantle interaction must have occurred in the form of isotopic exchange at the core-mantle boundary was confirmed in this study. However, any other mechanism proposed to be responsible for creating radiogenic $^{187}\text{Os}/^{188}\text{Os}$ in ancient komatiite mantle source regions must not affect the PGE abundances in the sources by a measurable amount, either. Studies of the Pt-Os systematics in Kostomuksha komatiites are required to further test this hypothesis.

Acknowledgments—We thank Thomas Meisel for sharing PGE results on UB-N, KAL-1 and other standards before publication, and Andy Campbell for support on the Element. We are grateful to Mark Rehkämper, Cin-Ty Lee, and Ed Mathez for constructive reviews, and to Ed Ripley for editorial handling. This study was supported by NSF EAR-0106974 and NSF EAR-0309786, which are gratefully acknowledged.

Associate editor: E. M. Ripley

REFERENCES

- Alard O., Griffin W. L., Lorand J. P., Jackson S. E., and O'Reilly S. Y. (2000) Non-chondritic distribution of the highly siderophile elements in mantle sulfides. *Nature* **407**, 891–894.
- Anders E. and Grevesse N. (1989) Abundances of the elements: Meteoritic and solar. *Geochim. Cosmochim. Acta* **53**, 197–214.
- Arndt N. T. (1976) Melting relations of ultramafic lavas (komatiites) at one atmosphere and high pressure. *J. Yb. Carnegie Inst. Wash.* **75**, 555–562.
- Arndt N. T., Naldrett A. J., and Pyke D. R. (1977) Komatiitic and iron-rich tholeiitic lavas of Munro Township, northeast Ontario. *J. Petrol.* **18**, 319–369.
- Barnes S.-J., Naldrett A. J., and Gorton M. P. (1985) The origin of the fractionation of platinum-group elements in terrestrial magmas. *J. Chem. Geol.* **53**, 303–323.
- Barnes S.-J., Leshner C. M., and Keays R. R. (1995) Geochemistry of mineralised and barren komatiites from the Perseverance nickel deposit, Western Australia. *Lithos* **34**, 209–234.
- Birck J. L., Roy-Barman M., and Capman F. (1997) Re-Os isotopic measurements at the femtomole level in natural samples. *Geostandards Newsletter* **20**, 19–27.
- Brügmann G. E., Arndt N. T., Hofmann A. W., and Tobschall H. J. (1987) Noble metal abundances in komatiite suites from Alexo, Ontario and Gorgona Island, Colombia. *Geochim. Cosmochim. Acta* **51**, 2159–2169.
- Cohen A. S. and Waters F. G. (1996) Separation of osmium from geological materials by solvent extraction for analysis by thermal ionisation mass spectrometry. *J. Anal. Chim. Acta* **332**, 269–275.
- Crocket J. H. and MacRae W. E. (1986) Platinum-group element distribution in komatiitic and tholeiitic volcanic rocks from Munro Township, Ontario. *Econ. Geol.* **81**, 1242–1251.
- Gangopadhyay A. and Walker R. J. (2003) Re-Os systematics of the ca. 2.7 Ga komatiites from Alexo, Ontario, Canada. *Chem. Geol.* **196**, 147–162.
- Green T. H. (1994) Experimental studies of trace-element partitioning applicable to igneous petrogenesis - Sedona 16 years later. *J. Chem. Geology* **117**, 1–36.
- Keays R. R. (1995) The role of komatiitic and picritic magmatism and S-saturation in the formation of ore deposits. *Lithos* **34**, 1–18.
- Leshner C. M. and Stone W. E. (1996) Exploration geochemistry of komatiites. In *Igneous Trace Element Geochemistry: Applications for Massive Sulphide Exploration*, Short Course, (ed. D. A. Wyman), pp. 153–204, Geological Association of Canada.
- Maier W. D., Roelofse F., and Barnes S.-J. (2003) The concentration of the platinum-group-elements in South African komatiites: Implications for mantle sources, melting regime and PGE fractionation during crystallization. *J. Petrol.* **44**, 1787–1804.
- Meisel T. and Moser J. (2004) Reference materials for geochemical PGE analysis: new analytical data for Ru, Rh, Pd, Os, Ir, Pt and Re by isotope dilution ICP-MS in 11 geological reference materials. *Chem. Geol.* **208**, 319–338.
- Morgan J. W. (1986) Ultramafic xenoliths: Clues to Earth's late accretionary history. *J. Geophys. Res.* **91**, 12375–12387.
- Pattou L., Lorand J. P., and Gros M. (1996) Non-chondritic platinum-group element ratios in the Earth's mantle. *Nature* **379**, 712–715.
- Pearson D. G., Irvine G. J., Ionov D. A., Boyd F. R., and Dreibus G. E. (2004) Re-Os isotope systematics and platinum-group-element fractionation during mantle melt extraction: A study of massif and xenolith peridotite suites. *J. Chem. Geol.* **208**, 29–59.
- Puchtel I. S. and Humayun M. (2000) Platinum group elements in Kostomuksha komatiites and basalts: Implications for oceanic crust recycling and core-mantle interaction. *Geochim. Cosmochim. Acta* **64**, 4227–4242.
- Puchtel I. S. and Humayun M. (2001) PGE fractionation in a komatiitic basalt lava lake. *Geochim. Cosmochim. Acta* **17**, 2979–2993.
- Puchtel I. S., Hofmann A. W., Mezger K., Jochum K. P., Shchipansky A. A., and Samsonov A. V. (1998) Oceanic plateau model for continental crustal growth in the Archaean: A case study from the Kostomuksha greenstone belt, NW Baltic Shield. *Earth Planet. Sci. Lett.* **155**, 57–74.
- Puchtel I. S., Brügmann G. E., and Hofmann A. W. (2001) ^{187}Os -enriched domain in an Archaean mantle plume: Evidence from 2.8

- Ga komatiites of the Kostomuksha greenstone belt, NW Baltic Shield. *Earth Planet. Sci. Lett.* **186**, 513–526.
- Puchtel I. S., Brandon A. D., and Humayun M. (2004a) Precise Pt-Re-Os isotope systematics of the mantle from 2.7-Ga komatiites. *Earth Planet. Sci. Lett.* **224**, 157–174.
- Puchtel I. S., Humayun M., Campbell A., Sproule R., and Leshner C. M. (2004b) Platinum group element geochemistry of komatiites from the Alexo and Pyke Hill areas, Ontario, Canada. *Geochim. Cosmochim. Acta* **68**, 1361–1383.
- Pyke D. R., Naldrett A. J., and Eckstrand O. R. (1973) Archean ultramafic flows in Munro Township, Ontario. *Geol. Soc. Amer. Bull.* **84**, 955–978.
- Rehkämper M., Halliday A. N., Alt J., Fitton J. G., Zipfel J., and Takazawa E. (1999a) Non-chondritic platinum-group element ratios in oceanic mantle lithosphere: petrogenetic signature of melt percolation? *Earth Planet. Sci. Lett.* **172**, 65–81.
- Rehkämper M., Halliday A. N., Fitton J. G., Lee D.-C., Wieneke M., and Arndt N. T. (1999b) Ir, Ru, Pt and Pd in basalts and komatiites: New constraints for the geochemical behavior of the platinum group elements in the mantle. *Geochim. Cosmochim. Acta* **63**, 3915–3934.
- Shaw D. M. (1970) Trace element fractionation during anatexis. *Geochim. Cosmochim. Acta* **40**, 73.
- Shirey S. B. and Walker R. J. (1995) Carius tube digestion for low-blank rhenium-osmium analysis. *J. Anal. Chem.* **67**, 2136–2141.
- Shirey S. B. and Walker R. J. (1998) The Re-Os isotope system in cosmochemistry and high-temperature geochemistry. *J. Ann. Rev. Earth Planet. Sci.* **26**, 423–500.
- Walker R. J. and Nisbet E. (2002) ^{187}Os isotopic constraints on Archean mantle dynamics. *Geochim. Cosmochim. Acta* **66**, 3317–3325.
- Walker R. J., Morgan J. W., and Horan M. F. (1995) ^{187}Os enrichment in some plumes: evidence for core-mantle interaction. *Science* **269**, 819–822.
- Zhou M. F. (1994) PGE distribution in 2.7-Ga layered komatiite flows from the Belingwe greenstone belt, Zimbabwe. *Chem. Geol.* **118**, 155–172.